AAS 07-112

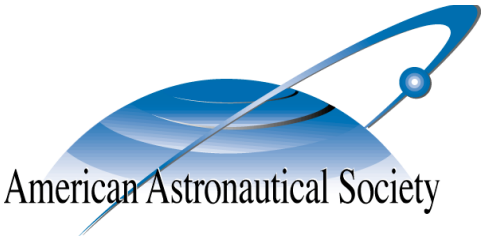

American Institute of
Aeronautics and Astronautics

SPACECRAFT COLLISION AVOIDANCE USING COULOMB FORCES WITH SEPARATION DISTANCE FEEDBACK

Shuquan Wang and Hanspeter Schaub

16th AAS/AIAA Space Flight Mechanics Meeting

Sedona, Arizona **Jan. 28–Feb. 1, 2007**

AAS Publications Office, P.O. Box 28130, San Diego, CA 92198

AAS 07-112

SPACECRAFT COLLISION AVOIDANCE USING COULOMB FORCES WITH SEPARATION DISTANCE FEEDBACK

Shuquan Wang* **and Hanspeter Schaub†**

A 2-spacecraft collision avoidance problem is discussed in this paper. The spacecraft are assumed to be floating freely in deep space. A control strategy using cluster internal Coulomb forces is developed to prevent a collision between two spacecraft. The control law is designed to keep the separation distance greater than a constraint value, and is also designed to keep the departure relative kinetic energy at the same level as the approach kinetic energy. Further, this strategy only requires measurements of the separation distances. If spacecraft charge saturation is also considered than it is not guaranteed that the collision can always be prevented. Conditions under which a collision can be avoided are discussed by formulating the charged spacecraft relative motion using concepts of orbital mechanics. Given an initial separation distance and distance rate, the minimum spacecraft charge limit required to guarantee collision avoidance is determined. Or, inversely, when the limitations of charges are given, the maximum approach speed at which a potential collision can be avoided is estimated. Numerical simulations illustrate the analytical results.

INTRODUCTION

Collision avoidance is a general concern in a tightly flying cluster of spacecraft with separation distances ranging on the order of dozens to hundreds of meters. Such mission concepts include small satellite swarms or close proximity flying scenarios where a smaller spacecraft is circumventing and inspecting a secondary craft. A spacecraft formation is a group or cluster of satellites flying with a specific shape or geometry. The spacecraft swarm concept envisions a large number of satellites flying relative to each other with loose position keeping requirements, while the swarm members provide a highly distributed and redundant sensor platform. Collisions can occur when spacecraft within the cluster have control or sensor failures, or lack the guidance strategy to guarantee collision avoidance among a large number of cluster members. Preventing collisions has many challenges. First, the collision onset must be sensed with sufficient accuracy to warrant a corrective maneuver. Second, a control strategy must be developed which can provide the required small corrective forces without causing plume impingement issues on neighboring satellites. This paper focuses on a mission scenario where a loose cluster of satellites are flying in deep space in a bounded configuration. The satellites are assumed to have a low approach speed with respect to each other. This strategy is not designed to repel high-velocity bodies.

A traditional approach to avoid collisions within a formation is to perform a velocity correction of the spacecraft as discussed in References 1 and 2. Slater in Reference 1 discusses the collision probability of a formation under the influence of orbital disturbances, and presents requirements for velocity corrections to avoid collision. Singh in Reference 2 considers a minimum effort collision avoidance strategy for a 2 spacecraft formation and develops a solution. This approach is labor intensive and becomes increasingly difficult to manage as the number of spacecraft in the formation

*Graduate student, Aerospace & Ocean Engineering Department, Virginia Tech, Blacksburg, VA
†Assistant Professor, Aerospace & Ocean Engineering Department, Virginia Tech, Blacksburg, VA.

increases. All the above approaches are based on the control strategies' capability to control all three components of the thrust vector in 3-D space. In addition, these control strategies use propellent, which will increase the fuel budget. Fuel efficient relative motion control is a critical factor for long term spacecraft cluster or swarm missions. Further, employing conventional thrusters when spacecraft are flying less than 100 meters apart is very challenging because of the associated thruster exhaust plume impingement issues.

This paper presents a new collision avoidance approach which uses only electrostatic (Coulomb) forces. Because the Coulomb force generation is essentially propellentless, it will not generate any propellent plume impingement issues that threaten neighboring spacecraft. Its application in spacecraft cluster flying has been studied frequently since Lyon B. King et al. originally discussed Coulomb Formation Flying (CFF) in Reference 3.

CFF uses Coulomb forces to control the distances between spacecraft to achieve the desired relative motion. The spacecraft charge level is actively controlled through the continuous emission of electrons or ions. Coulomb force control is 3-5 orders of magnitude more fuel-efficient than Electric Propulsion (EP) methods, and typically only require watt levels of electrical power to operate.[3] Whereas conventional thrusters can produce a thrust vector pointing in any direction, Coulomb forces only lie along the line-of-sight directions between the craft. Further, in space the spacecraft are not flying in a vacuum, but rather a sparse plasma environment which can shield electrostatic charges. The amount of shielding is controlled through the Debye length factor.[4,5] The cold and high-density plasma environment at LEO results in centimeter-length Debye lengths. This makes the use of Coulomb thrusting not feasible at low Earth orbit altitudes. However, at GEO the Debye lengths range between 100-1000 meters,[6,3] while at 1 AU in deep space they are around 20-40 meters.[3] This makes the Coulomb thrusting concept feasible for high Earth orbit altitudes and deep space missions where the minimum separation distances are less than 100 meters.

Both promising and challenging, many applications of Coulomb thrusting have been studied. The following papers discuss deep-space (i.e. no orbital motion) Coulomb thrusting applications. Gordon G. Parker et al. present a sequential control strategy for arranging N charged bodies into an arbitrary geometry using $N + 3$ participating bodies in Reference 7. Hussien et al. study shape-preserving spinning formations of three spacecraft in Reference 8. Inspired by the gravitational three-body problem, they derive general conditions for open-loop charges that guarantee preservation of the geometric shape of the rotating formation. Reference 9 is an example of an orbit based Coulomb proximity flying mission. Here a GEO chief satellite deploys deputy craft to specified end states. A multiple deputy deployment is designed by modulating the control authority across the formation. Feedback charge control strategies are discussed for the 2-craft GEO-based Coulomb tether concept in References 10 and 11. While this previous work investigates charge controlled relative motion between spacecraft, the collision avoidance problem is not directly addressed. Reference 12 discusses the concept of Coulomb thrusting and presents a semi-major axis based feedback strategy to use electrostatic forces to bounded the motion between 2 craft. Further, this paper discusses the potential of Coulomb thrusting to provide effective collision avoidance strategies. A numerical example illustrates that using a simple repulsive force field while at GEO will not guarantee a successful collision avoidance. Reference 12 does not provide any collision avoidance control strategy, it simply discusses the challenges and the potential of this Coulomb thrusting application.

This paper considers the first feedback control strategy using Coulomb thrusting to perform collision avoidance maneuvers. A potential collision of two spacecraft flying in deep space is considered where no external forces and torques are acting. A charge feedback control strategy is investigated

which maintains a desired minimum separation distance between 2 spacecraft. To minimize the sensor requirements, the control only requires separation distance measurements between the craft during the collision avoidance phase. The separation distance is much simpler to measure than the full six degree of freedom relative state vector.

A very simple concept to avoid a collision has both spacecraft charge up to large values of equal sign. The resulting repulsive force drives the craft apart, thus avoiding the collision. But this strategy also results in the 2 spacecraft flying apart at a considerable velocity, thus noticeably changing their inertial motion. This can cause sensing issues for the spacecraft themselves, but is also of concern if the 2 craft are operating within a larger cluster of spacecraft. This additional velocity makes future collision avoidance maneuvers more challenging. Instead the charge feedback control is developed with the additional goal to minimize changes to the relative kinetic energy level between the 2 craft.

Finally, the paper also considers the effect of charge saturation on the collision avoidance strategy. Even with sophisticated spacecraft designs there will always be a physical limit to which a craft can safely be charged. Of interest is determining how much initial approach speed the craft can have and still successfully avoid a collision. Analytical conditions are investigated to guarantee that a collision can be avoided if a given charge limit is considered.

Numerical simulations illustrate the performance of the developed collision avoidance control strategy. This simulations typically consider the craft to be operating in deep space. While the orbiting collision avoidance is not analytically considered in this paper, the numerical simulations do illustrate how the control performs if the spacecraft are not in deep space, but rather in an Earth geostationary orbit.

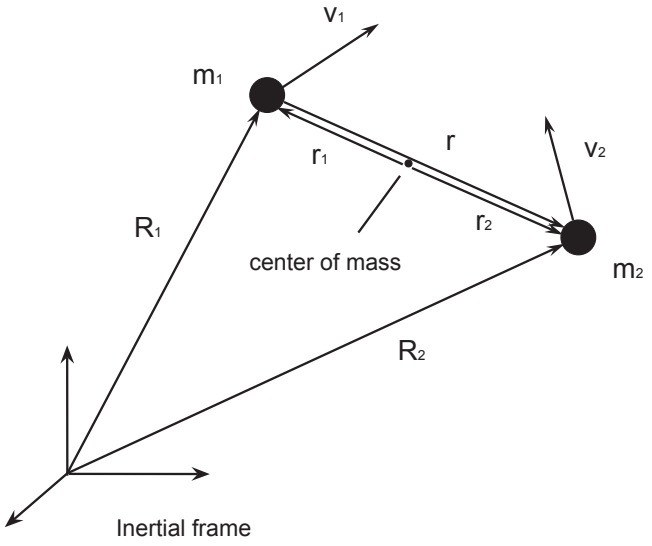

Figure 1 Illustration of the 2-spacecraft system.

CHARGED SPACECRAFT EQUATIONS OF MOTION

Consider two spacecraft flying in the free 3-dimensional space where there are no external forces acting on the system as shown in Figure 1. In CFF, the electrostatic forces directly control separation distance r and not the the inertial positions $\boldsymbol{R}_i$. And we are intending to use the separation distance

r and the distance rate $\dot{r}$ as the control feedback. So the separation distance equations of motion are required to develop a control strategy. The Coulomb force vector between the two spacecraft is

$$\boldsymbol{F} = -k_c \frac{q_1 q_2}{r^3} e^{-\frac{r}{\lambda_d}} \boldsymbol{r} = -k_c \frac{q_1 q_2}{r^2} e^{-\frac{r}{\lambda_d}} \hat{\boldsymbol{e}}_r \tag{1}$$

where $k_c = 8.99 \times 10^9 \mathrm{C}^{-2} \cdot \mathrm{N} \cdot \mathrm{m}^2$ is the Coulomb constant, r is the distance between the two spacecraft, $\boldsymbol{r} = \boldsymbol{R}_2 - \boldsymbol{R}_1$ is the relative position vector pointing of spacecraft 1 to spacecraft 2, $\hat{\boldsymbol{e}}_r$ is the unit vector of $\boldsymbol{r}$, and λ_d is the Debye length. The smaller the plasma Debye length is, the shorter the effective range is of a given electrical charge. For high Earth orbits the Debye length ranges between 100–1000 meters.[3,12,6] CFF concepts typically consider spacecraft separation distances ranging up to 100 meters.

The inertial equations of motion of the two spacecraft are

$$m_1 \ddot{\boldsymbol{R}}_1 = -k_c \frac{q_1 q_2}{r^2} e^{-\frac{r}{\lambda_d}} \hat{\boldsymbol{e}}_r \tag{2a}$$

$$m_2 \ddot{\boldsymbol{R}}_2 = k_c \frac{q_1 q_2}{r^2} e^{-\frac{r}{\lambda_d}} \hat{\boldsymbol{e}}_r \tag{2b}$$

where $\boldsymbol{R}_i$ is the inertial position vector of the i^{th} spacecraft. The inertial relative acceleration vector $\ddot{\boldsymbol{r}}$ is

$$\ddot{\boldsymbol{r}} = \ddot{\boldsymbol{R}}_2 - \ddot{\boldsymbol{R}}_1 = \frac{k_c q_1 q_2}{m_1 m_2 r^2} (m_1 + m_2) e^{-\frac{r}{\lambda_d}} \hat{\boldsymbol{e}}_r \tag{3}$$

where $\boldsymbol{r} = r\hat{\boldsymbol{e}}_r$. Taking a second time derivative yields the kinematic acceleration expression:

$$\ddot{\boldsymbol{r}} = (\ddot{r} - r\dot{\theta}^2)\hat{\boldsymbol{e}}_r + (2\dot{r}\dot{\theta} + r\ddot{\theta})\hat{\boldsymbol{e}}_\theta \tag{4}$$

Substituting Eq. (4) into (3) yields the scalar separation distance equation of motion:

$$\ddot{r} = r\dot{\theta}^2 + \frac{k_c Q}{m_1 m_2 r^2} (m_1 + m_2) e^{-\frac{r}{\lambda_d}} \tag{5}$$

Note that $2\dot{r}\dot{\theta} + r\ddot{\theta} = 0$ is a consequence of the inertial angular momentum being conserved with Coulomb forces. The term $Q = q_1 q_2$ is the charge product between the 2 spacecraft charges q_i. Because only the separation distance and distance rate will be fed back to the controller, $\dot{\theta}$ should be expressed in in terms of r, $\dot{r}$, and the initial conditions. This is accomplished by considering the angular momentum about the cluster center of mass.

The position vectors $\boldsymbol{r}_i$ of the two spacecraft with respect to the center of mass are

$$\boldsymbol{r}_1 = -\frac{m_2 r}{m_1 + m_2} \hat{\boldsymbol{e}}_r \tag{6a}$$

$$\boldsymbol{r}_2 = \frac{m_1 r}{m_1 + m_2} \hat{\boldsymbol{e}}_r \tag{6b}$$

The angular momentum $\boldsymbol{H}_c$ of the system about the center of mass is

$$\boldsymbol{H}_c = \boldsymbol{r}_1 \times \dot{\boldsymbol{r}}_1 m_1 + \boldsymbol{r}_2 \times \dot{\boldsymbol{r}}_2 m_2 = \frac{m_1 m_2}{m_1 + m_2} r^2 \dot{\theta} \hat{\boldsymbol{e}}_3 \tag{7}$$

Because there are no external torques acting on the system, the momentum vector $\boldsymbol{H}_c$ is conserved. So from $\boldsymbol{H}_c = \boldsymbol{H}_c(t_0)$, the angular rate $\dot{\theta}$ is derived

$$\dot{\theta} = \frac{r_o^2}{r^2}\dot{\theta}(t_0) = \frac{r_o}{r^2}\|\dot{\boldsymbol{r}}(t_0)\| \sin\alpha_0 = \left(\frac{1}{m_1} + \frac{1}{m_2}\right)\frac{\|\boldsymbol{H}_c(t_0)\|}{r^2} \tag{8}$$

where $\alpha_0 = \cos^{-1}\left(\frac{\dot{\boldsymbol{r}}(t_0)\cdot\boldsymbol{r}_o}{\|\dot{\boldsymbol{r}}(t_0)\|r_o}\right)$ is the angle between $\dot{\boldsymbol{r}}(t_0)$ and $\boldsymbol{r}_o$. Thus the separation distance equations of motion in Eq. (5) is rewritten as

$$\ddot{r} = \left(\frac{1}{m_1} + \frac{1}{m_2}\right)^2 \frac{\|\boldsymbol{H}_c(t_0)\|^2}{r^3} + \frac{\beta Q}{r^2}e^{-\frac{r}{\lambda_d}} \tag{9}$$

where $\beta = \frac{k_c(m_1+m_2)}{m_1 m_2}$. The collision avoidance control law challenge is to design the charge product Q such that the separation distance r satisfies a certain successful avoidance condition.

UNSATURATED CONTROL LAW

In order to develop a collision avoidance control law, an explicit statement describing the requirements is needed. A spacecraft (spacecraft 1) has a safe region $\mathfrak{B}_{r_s} = \left\{\boldsymbol{R}\middle|\|\boldsymbol{R} - \boldsymbol{R}_1\| \leq r_s\right\}$ which can not be penetrated at any time. Each spacecraft is monitoring relative motions of neighboring spacecraft. If another spacecraft (spacecraft 2) enters a certain region $\mathfrak{B}_{r_o} = \{\boldsymbol{R}|\|\boldsymbol{R} - \boldsymbol{R}_1\| \leq r_o\}$, named potential region, and is flying towards $\mathfrak{B}_{r_s}$, this relative motion is deemed as a potential collision. A control law is then triggered to prevent the potential collision. Here we consider a potential collision of only two spacecraft. Without loss of generality, we treat spacecraft 2 as a point mass moving towards $\mathfrak{B}_{r_s}$ of spacecraft 1. We can do this because the radius of the safe region of spacecraft 2 can be represented by adding it to the radius of the safe region of spacecraft 1.

The first and foremost goal of the control is to prevent the potential collision and drive spacecraft 2 out of the potential region $\mathfrak{B}_{r_o}$. That is to keep $r(t) \geq r_s$ for all time and make $r(t) > r_o$ in a finite time. Achievement of the first goal results in a successful collision avoidance. On the other hand, we don't want the final relative kinetic energy level changing too much compared with the original kinetic energy level. Our secondary goal of the control design is to maintain the kinetic energy level, that is to make $\dot{r}_{\text{final}} \approx |\dot{r}(t_0)|$ or to keep the changes bounded. Note that because only the separation distance is measure, not the full relative states, this condition will only achieve equal radial energy states.

If the trajectory of spacecraft 2 does not touch the ball $\mathfrak{B}_{r_s}$, no relative orbit correction is needed to avoid a collision. In this case the control strategy does not take effect. This situation is illustrated in Figure 2(a). Otherwise the electrostatic force fields are activated to repel the two spacecraft as shown in Figure 2(b).

Once spacecraft-2 enters $\mathfrak{B}_{r_o}$ and is moving towards $\mathfrak{B}_{r_s}$, the collision avoidance control is triggered. The term $x_1 = r(t) - r_o < 0$ represents how far spacecraft 2 has penetrated into the region $\mathfrak{B}_{r_o}$, and $x_2 = \dot{r}(t) + \dot{r}(t_0)$ represents the difference between the expected departure rate and the actual distance rate (note that $\dot{r}(t_0) < 0$). As stated above, the control law should reduce the absolute values of these two terms when $r(t) \leq r_o$. When $r(t) > r_o$, we have achieved a successful collision avoidance. Now the control is only trying to make $\dot{r}(t) \to -\dot{r}(t_0)$ to achieve the secondary goal, that is to maintain the radial relative kinetic energy level. Let us define the state

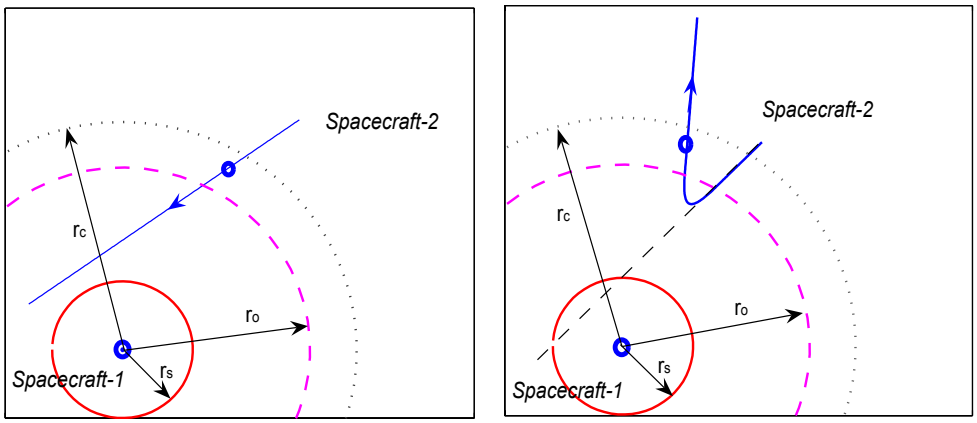

(a) Not a potential collision. (b) A potential collision.

Figure 2 Collision Avoidance Scenarios as Seen by the First Spacecraft.

vector $\boldsymbol{x} = (x_1, x_2)^T$ as

$$x_1 = \begin{cases} r(t) - r_o, & r(t) < r_o \\ 0, & r(t) \geq r_o \end{cases} \tag{10a}$$

$$x_2 = \dot{r}(t) + \dot{r}(t_0) \tag{10b}$$

Any final radial separation distance $r_{\text{final}} > r_o$ is acceptable, and is reflected with a zero x_1 state. If the 2nd spacecraft is outside of the region $\mathfrak{B}_{r_o}$ and the radial departure rate is the opposite of the radial approach rate, then both collision avoidance states x_i are zero. Thus the expected final states are $x_1(t_f) = 0$ and $x_2(t_f) = 0$. To successfully avoid a collision, the safety region penetration variable $x_1(t)$ can never be less than $r_s - r_o$. To achieve this behavior the Lyapunov function penalizing x_1 is designed to go to infinity when $x_1(t) = r_s - r_o$. Let us define a Lyapunov candidate function as

$$V = \frac{1}{2} k_1 \left(\frac{1}{x_1 - r_s + r_o} - \frac{1}{r_o - r_s} \right)^2 + \frac{1}{2} x_2^2 \tag{11}$$

where k_1 are positive coefficient. This function goes to infinity at safety boundary $x_1 \to r_s - r_o$ and if the radial separation rate grows unbounded. Note that even though x_1 is defined piecewise, it doesn't introduce a discontinuity in the Lyapunov function at $r(t) = r_o$. The first time derivative of the Lyapunov function is

$$\dot{V} = -k_1 \left(\frac{1}{x_1 - r_s + r_o} - \frac{1}{r_o - r_s} \right) \frac{\dot{x}_1}{(x_1 - r_s + r_o)^2} + x_2 \dot{x}_2 \tag{12}$$

Here we use $\dot{x}_2 = \ddot{r}$. The separation distance equation of motion in Eq. (9) relates the charge product Q with $\dot{V}$. In order to derive a control law from the Lyapunov function, we need to express $\dot{x}_1$ in terms of some known variables. From the definition of x_1, it is obvious that $\dot{x}_1 = x_2 - \dot{r}(t_0)$ when $r(t) < r_o$. But $\dot{x}_1 \neq x_2 - \dot{r}(t_0)$ when $r(t) \geq r_o$.

Note that $\left(\frac{1}{x_1 - r_s + r_o} - \frac{1}{r_o - r_s} \right)$ is zero when $r(t) \geq r_o$, so the first term in Eq. (12) is zero when $r(t) \geq r_o$, no matter what $\dot{x}_1$ is. Thus we can globally replace $\dot{x}_1$ with $x_2 - \dot{r}(t_0)$ in the first term

of Eq. (12) and simplify $\dot{V}$ to:

$$\dot{V} = -k_1 \left(\frac{1}{x_1 - r_s + r_o} - \frac{1}{r_o - r_s} \right) \frac{x_2 - \dot{r}(t_0)}{(x_1 - r_s + r_o)^2} + x_2 \ddot{r}(t) \tag{13}$$

Note that $\dot{V}$ is continuous and well defined for all ranges of the separation distance r. Now we can directly substitute the separation distance equation of motion in Eq. (9) into $\dot{V}$ to design a charge feedback control law Q using Lyapunov's direct method.

Assume a charge control law with feedback of separation distance and separation distance rate as

$$Q = \frac{k_1}{\beta} \left(\frac{1}{x_1 - r_s + r_o} - \frac{1}{r_o - r_s} \right) \frac{r(t)^2}{(x_1 - r_s + r_o)^2} e^{\frac{r}{\lambda_d}} - \frac{k_2}{\beta} r(t)^2 x_2 e^{\frac{r}{\lambda_d}} \tag{14}$$

Using the Lyapunov function V in Eq. (11), and substituting the charge control in Eq. (14) into the equations of motion in Eq. (9), we differentiate V to find the Lyapunov function rate expression:

$$\dot{V} = k_1 \left(\frac{1}{x_1 - r_s + r_o} - \frac{1}{r_o - r_s} \right) \frac{\dot{r}(t_0)}{(x_1 - r_s + r_o)^2} - k_2 x_2^2 + x_2 \left(\frac{1}{m_1} + \frac{1}{m_2} \right)^2 \frac{\|\boldsymbol{H}_c\|^2}{r^3} \tag{15}$$

Note that $\left(\frac{1}{x_1 - r_s + r_o} - \frac{1}{r_o - r_s} \right) \geq 0$, and it equals zero when $x_1 = 0$. Because $\dot{r}(t_0) < 0$ the first term in Eq. (15) cannot be positive. Thus the Lyapunov function rate is bounded by

$$\dot{V} \leq -k_2 x_2^2 + x_2 \left(\frac{1}{m_1} + \frac{1}{m_2} \right)^2 \frac{\|\boldsymbol{H}_c\|^2}{r^3} \tag{16}$$

Because $\left(\frac{1}{m_1} + \frac{1}{m_2} \right)^2 \frac{\|\boldsymbol{H}_c\|^2}{r^3} > 0$, from Eq. (16) we find that $\dot{V} < 0$ if

$$x_2 > \frac{1}{k_2} \left(\frac{1}{m_1} + \frac{1}{m_2} \right)^2 \frac{\|\boldsymbol{H}_c\|^2}{r^3} \quad \text{or} \quad x_2 < 0 \tag{17}$$

Let us define the scalar function $b(r)$ as

$$b(r) = \frac{1}{k_2} \left(\frac{1}{m_1} + \frac{1}{m_2} \right)^2 \frac{\|\boldsymbol{H}_c\|^2}{r^3} \tag{18}$$

The condition in Eq. (17) and the $\dot{V}$ bound in Eq. (16) show that the charge product Q in Eq. (14) will make x_2 converge to the interval $[0, b(r)]$.

Now let us investigate what occurs with the collision separation state x_1 under this charge control law. The radial rate error state x_2 starts with $2\dot{r}_0 < 0$, and $\dot{V}$ starts as well with a negative value. As long as $x_2 < 0$, Q will keep driving $x_2 \to 0$ asymptotically because $\dot{V} < 0$ in this situation.

If x_2 crosses zero to enter the positive interval $(0, b(r))$ then $\dot{V}$ becomes positive. Eq. (17) shows that the only chance for V to go to infinity is that x_2 remains bounded and stays in $(0, b(r))$ for an infinite time. However, note that when $x_2 \in (0, b(r))$, x_1 is increasing and $x_1 \not\to r_s - r_o$. According to Eq. (11), if x_2 is bounded and $x_1 \geq r_s - r_o$, V is bounded too. So V can never go to infinity.

Observing the definition of V in Eq. (11) again, we find that if the craft approach too closely with $x_1 \leq r_s - r_o$, then the Lyapunov function V must have gone to infinity. Because V is always

bounded, the state x_1 won't violate $r_s - r_o$ even when $\dot{V} > 0$. This also means that the separation distance $r(t)$ will never violate the restraint separation distance r_s. Because r will reach r_o in a finite time without violating the constraint $r \geq r_s$, we can conclude that the charge control law Q in Eq. (14) guarantees a successful collision avoidance.

Though x_2 converges to the interval $[0, b(r)]$ asymptotically, it's not guaranteed that x_2 will converge to zero. If $\boldsymbol{H}_c = 0$, the interval shrinks to the zero point, thus x_2 converges to zero asymptotically. Otherwise, let us analyze the properties of x_2 a little further.

We have shown that x_1 will converge to zero in a finite time and stay there, and x_2 is approaching the interval $[0, b(r)]$ from an initial negative value. When x_2 reaches zero, if $x_1 = 0$, then the charge product $Q = 0$. By the separation distance equations of motion in Eq. (9), x_2 increases in this scenario because $\|\boldsymbol{H}_c\| > 0$. Thus x_2 enters the open interval $(0, b(r))$. Because $\dot{V}$ is positive when x_2 stays in the open interval, x_2 will be driven to increase until it reaches $b(r)$. Because $\dot{V} < 0$ when $x_2 > b(r)$, in this case x_2 converges to $b(r)$. If $x_1 < 0$ when x_2 reaches zero, because x_1 will converge to zero in a finite time, then after that finite time, x_2 is going to converge to $b(r)$. Now we can conclude that when $\boldsymbol{H}_c \neq 0$, x_2 will converge to $b(r)$. Note that $b(r) \to 0$ as $r \to \infty$, thus $x_2 \to 0$ as $r \to \infty$.

Practically speaking the range of the electrostatic control is limited due to the drop off of the Coulomb field strength. As a result, the controller will be turned off after the state goes inside a certain deadzone region. Let us define a radius $r_c > r_o$ where the collision avoidance charge control is turned off. The effect of this limitation is a termination of the control when $x_1 = 0$ and $r(t) > r_c$. Note that when the truncation happens, the potential collision has been successfully avoided. After the control charges are turned off, there are no forces acting on the spacecraft. The two spacecraft are now flying freely in space (by the assumption that the spacecraft are flying in free space) with constant velocities. The separation distance is still bounded, even though it's not converging to the magnitude of the approach rate.

Given the charge product in Eq. (14) to produce the required electrostatic force field, the individual spacecraft charges q_i are evaluated through

$$q_1 = \sqrt{|Q|} \tag{19}$$

$$q_2 = \text{sign}(Q) q_1 \tag{20}$$

There are an infinity of choices how Q can be mapped into q_1 and q_2. This strategy evenly distributed the charge amount across both craft. If one craft can handle a higher charge level, this can easily be taken into account.

SATURATED COLLISION AVOIDANCE ANALYSIS

Without saturation of spacecraft charges, the controller presented in the previous section works well in preventing a potential collision. But this is only the ideal case. The spacecraft charge magnitudes are always limited. The ability of the two-body system to prevent a potential collision is reduced compared with the non-saturated control law. For example, if the approach speed is too large the spacecraft saturated charge may not generate a force large enough to prevent a collision.

This section discusses limited charge control requirements for a collision to be preventable. When the two spacecraft are fully charged such that the charge product reaches its maximum positive value, the two craft are doing their best effort to avoid the collision by generating the largest possible

repulsive electrostatic forces. In this case, if the distance r still decreases to be less than the safety restraint distance r_s, we say that the collision is not avoidable. Otherwise, the collision is avoidable.

Constant Charge Spacecraft Equations of Motion

Our discussion of the conditions for a potential collision to be avoidable is based on the assumptions that the charge product remains at its maximum value $Q = Q_{\max} > 0$ to generate the largest repulsive force. The Coulomb force in Eq. (1) simplifies to be

$$\boldsymbol{F} = -k_c \frac{Q_{\max}}{r^3} e^{-\frac{r}{\lambda_d}} \boldsymbol{r} \tag{21}$$

and the inertial relative motion is

$$\ddot{\boldsymbol{r}} = \beta \frac{Q_{\max}}{r^3} e^{-\frac{r}{\lambda_d}} \boldsymbol{r} \tag{22}$$

Note that the form of the Coulomb force is very similar to the gravity force, this makes it possible to describe the motion using the formulas of the gravitational 2-body problem (2BP). Reference 8 provides us an approach to analyze this Coulomb forced spacecraft motion using 2BP method. In order to apply a 2BP method in analyzing our Coulomb forced motion, we need to find the radial equation and the energy equation in a similar form as in 2BP. Let us introduce the effective gravitational parameter

$$\mu(r) = -k_c \frac{Q_{\max}(m_1 + m_2)}{m_1 m_2} e^{-\frac{r}{\lambda_d}} \tag{23}$$

Next, assume the plasma Debye length interaction is weak and that $r \ll \lambda_d$. Then $e^{-\frac{r}{\lambda_d}} = 1$ and the parameter $\mu(r)$ becomes a constant

$$\mu = -k_c \frac{Q_{\max}(m_1 + m_2)}{m_1 m_2} \tag{24}$$

The relative equation of motion reduces to the familiar 2BP form

$$\ddot{\boldsymbol{r}} = -\frac{\mu}{r^3} \boldsymbol{r} \tag{25}$$

Eq. (25) has the same form as the equation of motion of the gravitational two-body problem (2BP), except that here μ is a negative number with $Q_{\max} > 0$. By assuming $r \ll \lambda_d$, μ becomes a constant, so the orbit radial trajectory is a conic section curve. Because $\mu < 0$ for the repulsive force case, all relative trajectories are hyperbolas where craft 2 orbits the un-occupied focus.[8] The signs of some parameters of the conic section are different from that of the gravitational 2BP. In our case, because $\mu < 0$, the semi-latus radium $p < 0$ and the semi-major axis $a > 0$.

Because of the hyperbolic motion about the un-occupied focus, the radial equation is also different from that of the gravitational 2BP:[8]

$$r = \frac{p}{1 - e\cos f} \tag{26}$$

Here the semi-latus rectum $p = h^2\mu < 0$, and h is the magnitude of the massless angular momentum $\boldsymbol{h} = \boldsymbol{r} \times \dot{\boldsymbol{r}}$. The energy equation is derived in the same procedure as the 2BP, and yields an identical equation:

$$\frac{v^2}{2} - \frac{\mu}{r} = -\frac{\mu}{2a} \tag{27}$$

where v is the magnitude of velocity vector $\dot{\boldsymbol{r}}$ and

$$v^2 = \dot{\boldsymbol{r}} \cdot \dot{\boldsymbol{r}} = \dot{r}^2 + (r\dot{f})^2 = \dot{r}^2 + \frac{h^2}{r^2} \tag{28}$$

Here $\dot{f}$ is the in-plane rotation rate.

Because the total energy is positive, the relative trajectory of the two spacecraft is a hyperbola. As seen by spacecraft 1, spacecraft 2 is traveling along the hyperbola, and spacecraft 1 is standing at the unoccupied focus point[8] as illustrated in Figure 3.

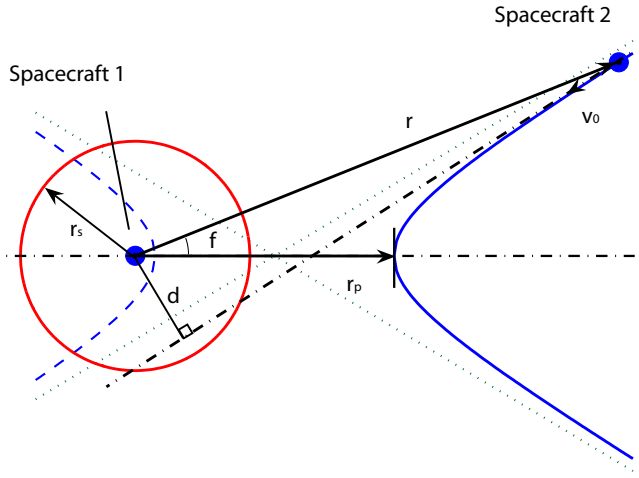

Figure 3 Illustration of the 2-Body hyperbolic trajectory.

From Eq. (26), the closest separation distance corresponds to $r(f = 0)$ which is the radius of periapsis

$$r_p = \frac{p}{1-e} = a(1+e) \tag{29}$$

Thus, given an initial spacecraft approach speed, the criterion for a successful collision avoidance is to determine a required saturated charge level which guarantees that

$$r_p \geq r_s \tag{30}$$

Avoidance Analysis

When $h \neq 0$ for the dynamical system, there exists an offset d between the position of spacecraft 1 and the direction of the relative velocity of spacecraft 2, as shown in Figure 3. Note that we are

assuming here that the current flight path will result in a potential collision where r will become less than r_s. The massless angular momentum is represented in terms of d and v_0:

$$h = \|\boldsymbol{r}_o \times \dot{\boldsymbol{r}}(t_0)\| = dv_0 \tag{31}$$

Using this expression instead of expressing h in terms of $\dot{r}(t_0)$ and $\dot{\theta}$, we can avoid the complexity brought by adding up two orthogonal velocity vector components $\dot{r}(t_0)\hat{\boldsymbol{e}}_r$ and $r\dot{\theta}\hat{\boldsymbol{e}}_\theta$. The states v_0 and d are evaluated by

$$v_0 = \sqrt{\dot{r}(t_0)^2 + (r_o\dot{f}_0)^2} \tag{32}$$

$$d = \frac{r_o^2\dot{f}_0}{v_0} \tag{33}$$

Because the angular momentum is conserved during the electrostatic collision avoidance maneuver as with the 2BP, the relation between the angular momentum and the orbit elements is:

$$h^2 = \mu a(1 - e^2) \tag{34}$$

Solving for the eccentricity e yields

$$e = \sqrt{1 - \frac{h^2}{\mu a}} \tag{35}$$

This e formulation can be used to calculate the periapses radius r_p:

$$r_p = a(1 + e) = a + \sqrt{a^2 - \frac{ah^2}{\mu}} \tag{36}$$

The collision avoidance criteria $r_p \geq r_s$ yields the condition

$$a + \sqrt{a^2 - \frac{ah^2}{\mu}} \geq r_s \tag{37}$$

Subtracting a from both sides and squaring the result yields

$$-\frac{ah^2}{\mu} \geq r_s^2 - 2ar_s \tag{38}$$

Now we need to determine the semimajor axis a to obtain the relationship between μ and the initial states of the system. From the energy equation in Eq. (27) we can solve for a:

$$a = \frac{r_o\mu}{2\mu - r_o v_0^2} \tag{39}$$

Substituting Eq. (39) into Eq. (38), and using $h = v_0 d$, yields

$$-\frac{r_o v_0^2 d^2}{2\mu - r_o v_0^2} \geq r_s^2 - \frac{2r_o r_s \mu}{2\mu - r_o v_0^2} \tag{40}$$

Note that $2\mu - r_o v_0^2 < 0$. Multiplying both sides by $-(2\mu - r_o v_0^2)$ results in

$$r_o v_0^2 d^2 \geq r_s^2 r_o v_0^2 + 2r_s(r_o - r_s)\mu \tag{41}$$

Eq. (41) shows the relationship of d, v_0 and μ for an avoidable collision. Solving Eq. (41) for μ, and using the definition of μ in Eq. (24), we obtain the maximum required charge criteria to avoid a collision with a given initial approach speed v_0 and miss-distance d.

$$Q_{\max} \geq \frac{m_1 m_2}{m_1 + m_2} \frac{r_o v_0^2 (r_s^2 - d^2)}{2k_c r_s (r_o - r_s)} \tag{42}$$

For example, a large value of $\dot{r}(t_0)^2$ means spacecraft 2 is approaching spacecraft 1 at a high speed. Here v_0 is large and according to Eq. (42) a large $Q_{\max}$ is required to avoid the collision. If the upper limit of the initial separation distance rate $\dot{r}(t_0)$ is known, Eq. (42) tells us the minimum value of the saturated charge product to avoid the collision successfully. For a given formation flying mission where the maximum magnitude of the possible separation distance rate has been determined, Eq. (42) helps us design the electric charge devices of the Coulomb forced spacecraft to provide the maximum required repulsive forces.

Alternatively, solving Eq. (41) for v_0 we obtain the criterion for the magnitude of the relative velocity:

$$v_0 \leq \sqrt{\frac{2\mu r_s (r_o - r_s)}{r_o (d^2 - r_s^2)}} \tag{43}$$

If parameter μ of the spacecraft is given (specifically maximum spacecraft charge is given), then Eq. (43) tells us the maximum allowable relative velocity that guarantees the collision to be avoidable. As expected, the small the allowable charge levels, the smaller the allowable approach speeds v_0 are.

To provide insight into the maximum charge and initial velocity relationship, Figure 4 shows the critical surface of parameters d, v_0 and $Q_{\max}$ under the following conditions:

$$\begin{cases} m_1 = 50\text{kg} \\ m_2 = 50\text{kg} \end{cases}, \qquad \begin{cases} r_s = 4\text{m} \\ r_o = 18\text{m} \end{cases} \tag{44}$$

Parameters d, v_0 and $Q_{\max}$ in the region above the critical surface represent avoidable collisions. Beneath the surface are parameters of unavoidable collisions.

This critical surface is one quarter of a saddle surface. When the magnitude of the relative velocity v_0 is set, the larger the offset d is, the smaller $Q_{\max}$ is required. And when $d = r_s$, $Q_{\max} = 0$, the trajectory of spacecraft 2 will touch the safe region of spacecraft 1 $\mathfrak{B}_{r_s}$ but won't penetrate it without any control. If the offset d is set, the larger v_0 results in the bigger $\dot{r}_0$ component, thus the larger $Q_{\max}$ is required for a successful collision maneuver. When $v_0 = 0$, which means the two spacecraft are stationary to each other, nothing needs to be done to avoid a collision, so $Q_{\max}$ in this case remains zero.

When $h = 0$, then the offset $d = 0$ and the craft are lined up for a head-on collision. For this worst case situation the criterions in Eq. (42) and Eq. (43) reduce to

$$Q_{\max} \geq \frac{\dot{r}(t_0)^2}{2k_c} \frac{m_1 m_2}{m_1 + m_2} \frac{r_o r_s}{r_o - r_s} \tag{45}$$

$$\dot{r}(t_0)^2 \leq 2\mu \left(\frac{1}{r_o} - \frac{1}{r_s} \right) \tag{46}$$

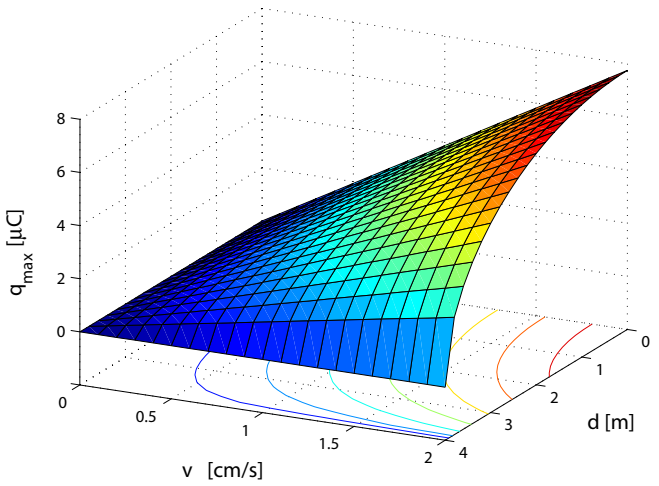

Figure 4 Critical surface of parameters for an avoidable collision.

Note that even though the derivation of the criterions are based on the assumption that $Q = Q_{\max} > 0$ and $d < r_s$, the same procedure can also be performed in the case $Q = Q_{\min} < 0$ and $d > r_s$. In this case, two spacecraft are attracting each other. The problem is then changed to be analyzing requirements for two attracting spacecraft not to collide. After the same procedure as we done above in this section, we get

$$Q_{\min} \geq \frac{m_1 m_2}{m_1 + m_2} \frac{r_o v_0^2 (r_s^2 - d^2)}{2 k_c r_s (r_o - r_s)} = g \tag{47}$$

Eq. (47) has exactly the same form as Eq. (42). Because $d > r_s$, here $g < 0$. It's assumed that the two spacecraft are attracting each other, the charge product Q is always negative. The smaller Q is, the larger the attracting force becomes, and thus the more likely the two spacecraft will get closer. If in a mission the two spacecraft are fully charged such that $Q = Q_{\min}$, then Eq. (47) tells us the minimum allowable value of the limit of the negative charge product Q guaranteeing that the spacecraft won't collide.

NUMERICAL SIMULATIONS

While the charge control is derived for general 3D spacecraft motion, the conservation of angular momentum forces all resulting motion to be planar. Thus, without loss of generality, the following numerical simulation all consider planar motion to simplify the visualizations.

The masses of the two spacecraft are $m_1 = m_2 = 50$kg. We assume at first that the spacecraft are flying in the deep space with the Debye length being $\lambda_d = 50$m. The radii of the safe region r_s and the potential region r_o determined by the requirements of a specific formation mission. For these simulations we set r_s and r_o as

$$r_s = 3\text{m}, \quad r_o = 16\text{m}.$$

The region of the effective control range r_c will be given in specific simulation examples. The initial inertial coordinates and inertial velocities are

$$\begin{array}{ll} \boldsymbol{R}_1 = [-8, -3]^T \text{m} & \dot{\boldsymbol{R}}_1 = [0.0060.002]^T \text{m/s} \\ \boldsymbol{R}_2 = [8, 3]^T \text{m} \quad , & \dot{\boldsymbol{R}}_2 = [-0.006 - 0.002]^T \text{m/s} \end{array} \tag{48}$$

These initial conditions are setup such that the spacecraft cluster center of mass is stationary.

Simulation without control truncation or charge saturations

The charge control law in Eq. (14) is guaranteed to prevent any potential collision. As to the coefficients of the controller, the larger k_1 is, the more we penalize the spacecraft proximity near r_s. And larger k_2 results in more effort in driving $\dot{r}$ to $-\dot{r}(t_0)$. For the first simulation the coefficients as $k_1 = 0.000001\text{kgm}^4\text{s/C}^2$, $k_2 = 0.0002\text{s/C}$ are chosen. Using these coefficients we study a case where the state x_2 crosses zero and then converge to $b(r)$. Figure 5 shows the numerical simulation results in the initial conditions listed above. Note that here the effective control range r_c is set to be infinity and no control truncation is occurring. The spacecraft 1 and spacecraft 2 start from a separation distance slightly larger than r_o. Before $r(t) = r_o$, the control is not triggered and the charges remain zero. When $r(t) = r_o$, the control is triggered and the spacecraft start to repel each other. After about 1.3 hours we find that $r(t) > r_o$, and the control law is only trying to equalize the radial separation rate with the initial value. The collision has been successfully avoided. The following discussion illustrates the analytical predictions of the x_2 behavior.

From our analysis x_2 will converge to the interval $[0, b(r)]$. Further, it will eventually converge to $b(r)$ if it crosses zero. Figure 5(d) and 5(e) show the history of the separation distance rate. After x_2 crosses zero, it keeps rising up as predicted. Figure 5(e) shows that x_2 crosses $b(r)$ at point A. At this critical point $\dot{V} = 0$ and $x_2 = b(r) > 0$. Using Eq. (14) we can solve the charge product $Q = -\frac{\|\boldsymbol{H}_c\|^2}{k_c r} e^{\frac{r}{\lambda_d}}$. From the separation distance equation of motion in Eq. (9), we can get the acceleration of the separation distance $\ddot{r} = 0$. Note that $\dot{x}_2 = \ddot{r}$, thus x_2 stops increasing at point A, and starts to decrease. At point A, $\dot{x}_2 = 0$, and x_2 is bounded by b function value at point A. So x_2 crosses the history of $b(r)$ because $b(r)$ is decreasing. After x_2 hits $b(r)$, it converges to the history of $b(r)$ asymptotically because $\dot{V} < 0$.

Figure 5(f) shows that after 15 hours the spacecraft attract each other to make x_2 converge to $b(r)$. In Figure 5(e) this is when the state x_2 becomes positive. Physically this means that the separation rate is now larger than the original radial approach rate magnitude. To slow down the radial motion, the charge signs become opposite to yield attractive forces. The reason the charge values are increasing here is because the separation distances have already grown very large here. Even though the required control force is very small, the $1/r^2$ dependency of the Coulomb force expression requires a large spacecraft charge to generate it. This issue has little to no practical consequence. The collision avoidance maneuver was effectively finished after about 1.3 hours. This long term behavior is simply provide to numerical illustrate the analytically predicted x_2 behavior.

When the controller's coefficients are set as $k_1 = 0.0002$ kgm^{4}s/C^2, and $k_2 = 0.0001$ s/C, the state x_2 won't reach zero, but still converge asymptotically to zero from a negative value. Figure 6 shows the simulation results under these conditions. As shown in Figure 6(d), because k_1 is large, the control charges penalizing the spacecraft proximity near r_s dominate in the initial hour. The charge peak happens when the two spacecraft get closest. Physically when the craft get close, the repulsive force suddenly increases to a peak to repel the craft. This results in a sharp trajectory of the spacecraft as shown in Figure 6(a).

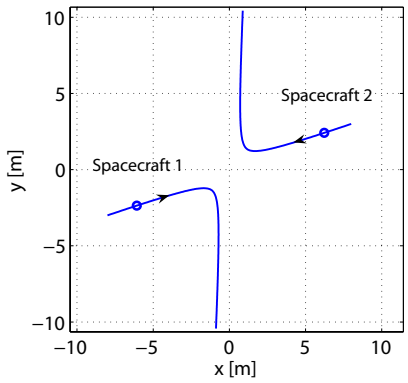

(a) inertial scenario

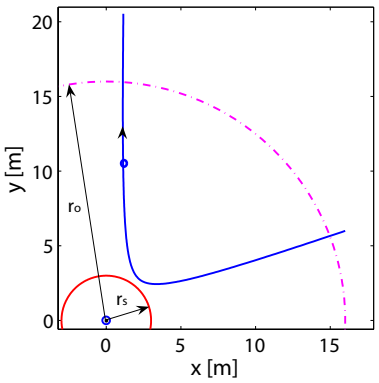

(b) scenario as seen from spacecraft 1

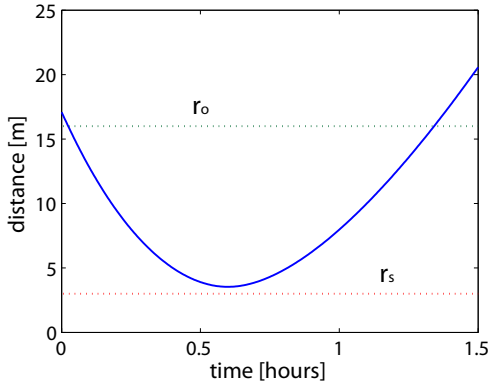

(c) separation distance history

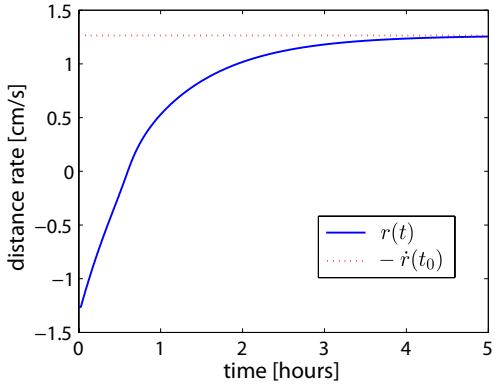

(d) separation distance rate

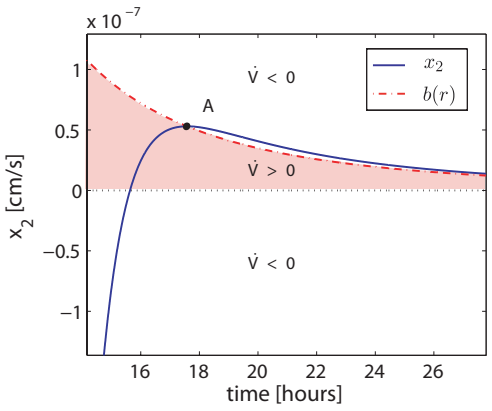

(e) illustration of the convergence of x_2 to $b(r)$

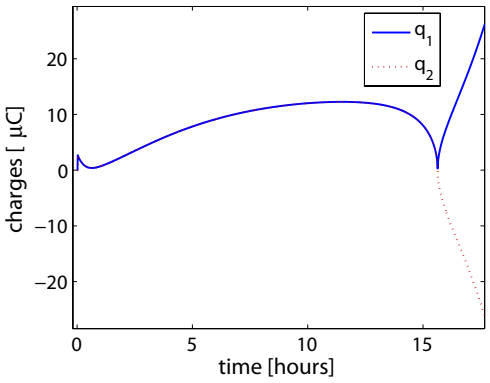

(f) spacecraft charges q_1&q_2

Figure 5 Simulation results without truncation and charge saturations, in the case that x_2 crosses zero.

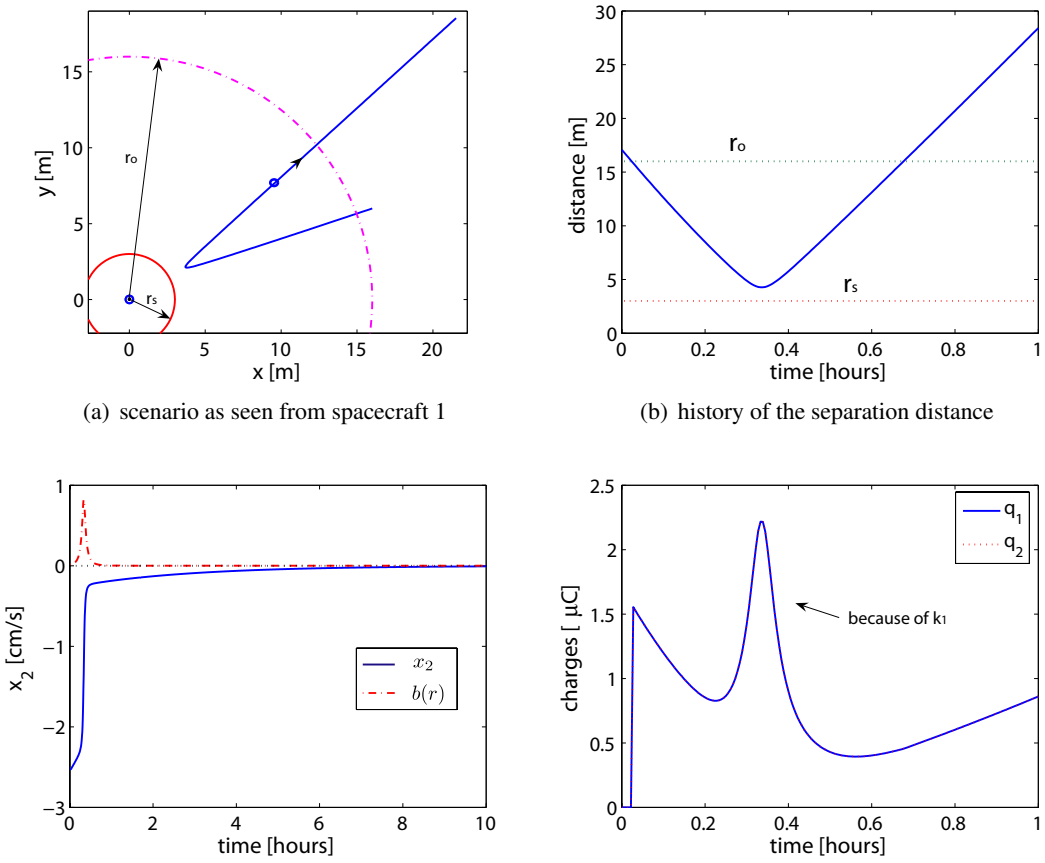

(a) scenario as seen from spacecraft 1

(b) history of the separation distance

(c) history of the separation distance rate

(d) history of charges q_1

Figure 6 Simulation results without truncation and charge saturations, in the case that x_2 won't cross zero.

Simulation with charge truncations

In the following simulations the control is truncated if the separation distance is larger than $r_c > r_o$. The range of the control is denoted by $\mathfrak{B}_{r_c}$ with radius r_c. The control charges will be turned off when the separation distance $r(t) > r_c$. Setting $r_c = 20$m, $k_1 = 0.0001$ kgm^{4}s/C^2, $k_2 = 0.0003$ s/C and using the previous spacecraft initial position and velocity conditions, Figure 7 shows simulation result this case.

Because of the truncations, we cannot guarantee that x_2 will converge to zero during this maneuver. However, as the control analysis predicted the x_2 radial rate tracking error will remain bounded while yielding a successful collision avoidance maneuver where $x_1 \to 0$.

In order to test the robustness of the control, the spacecraft are put in an geostationary orbit to compare the performance with that of the spacecraft flying in deep space. The initial conditions in Eq. (48) are treated as LVLH frame position and velocity vectors, which are then mapped into inertial vectors with respect to the Earth centered inertial frame. The full nonlinear equations of motion are then integrated with the same charge collision avoidance control applied. After the

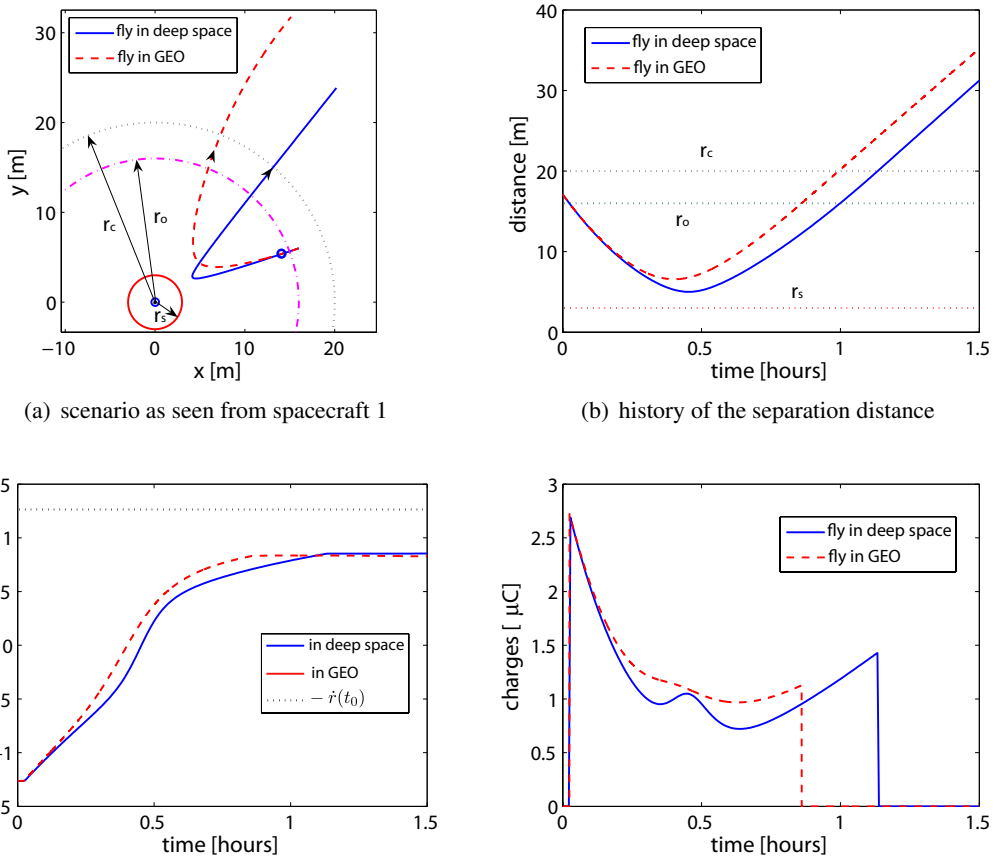

(a) scenario as seen from spacecraft 1

(b) history of the separation distance

(c) history of the separation distance rate

(d) history of charges q_1

Figure 7 Simulation results with truncation but without charge saturations.

integration the resulting motion is mapped back into equivalent LVLH frame position vectors, where the rotating LVLH frame is assumed to be the spacecraft cluster center of mass. The simulation results are illustrated in Figure 7 simultaneously with the simulation performed in deep space.

The parameters of the two spacecraft and the controller are the same. In GEO the Debye length ranges from 100-1000 meters. But for a fair comparison, here we still use $\lambda_d = 50$m. While the trajectories in Figure 7(a) are different for the deep space and GEO cases, they both yield a separation distance $r(t)$ is always greater than safety limit r_s. From the charge control law in Eq. (14), the charge product Q will increase if $r(t)$ gets too close to r_s. In fact, we find that $Q \to \infty$ if $r(t) \to r_s$. Thus, while orbital motion has not been analytically considered in this paper, the presented unsaturated collision avoidance strategy does successfully maintain a specified safety distance r_s.

Simulation with charge saturations

When spacecraft charge saturation is introduced, a potential collision will be unpreventable if the two spacecraft are flying towards each other at a very high speed. Eq. (42) and (43) provide

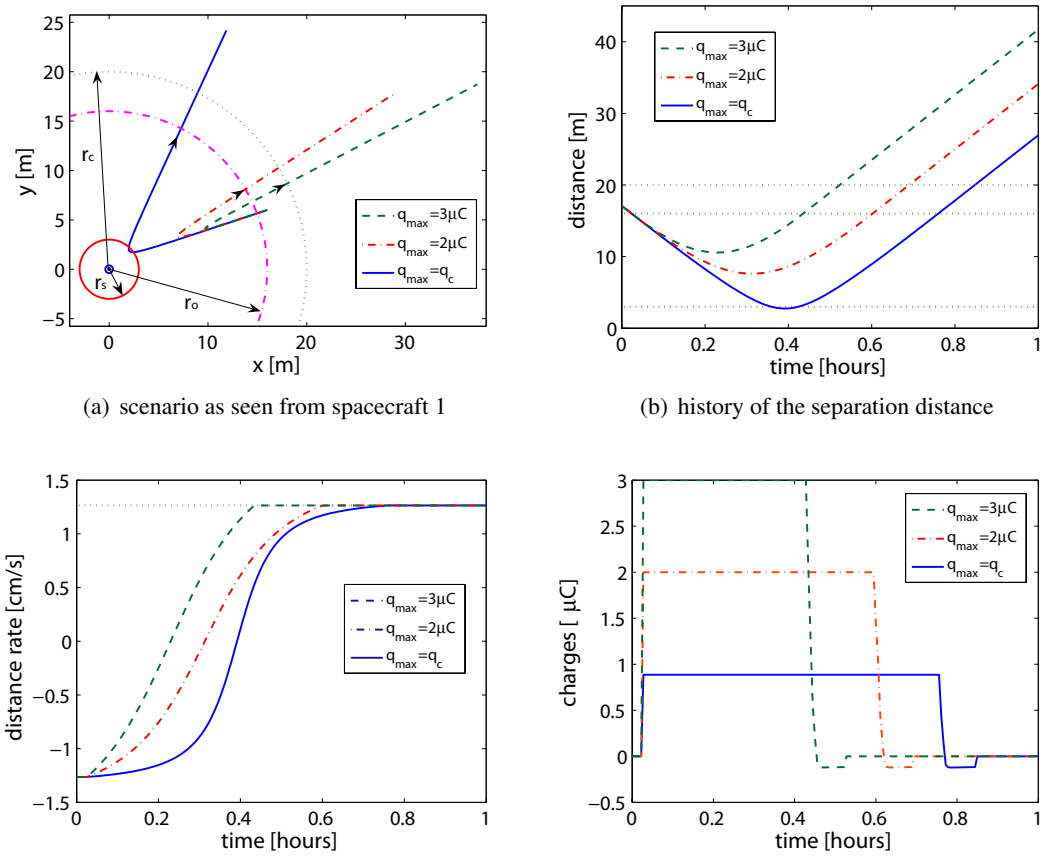

(a) scenario as seen from spacecraft 1

(b) history of the separation distance

(c) history of the separation distance rate

(d) history of charges q_1

Figure 8 Simulation results with charge saturation.

the criterion for an avoidable potential collision. Note that even though our analysis of avoidable collision is based on the assumption that the Debye length $\lambda_d \to \infty$, here in our simulation the Debye length is still set to be $\lambda_d = 50$m to show how close the estimation in Eq. (42) is with a limited Debye length. With the same initial conditions as in the previous simulation examples in Eq. (48), the initial offset distance d and the magnitude of initial relative velocity v_0 are

$$d = 0.6325\text{m}, \qquad v_0 = 0.0126\text{m/s}$$

Utilizing r_s, r_o and masses m_i, the critical charge product for an avoidable collision is

$$Q_{\text{C}} = \frac{m_1 m_2}{m_1 + m_2} \frac{r_o v_0^2 (r_s^2 - d^2)}{2 k_c r_s (r_o - r_s)} = 7.8492 \times 10^{-13} \text{C}^2 \tag{49}$$

The critical saturation limit for individual charge is $q_c = \sqrt{Q_{\text{C}}} = 0.88596\ \mu$C.

Figure 8 shows simulations with the same initial conditions but different charge saturation limits. It is assumed that in the potential region $\mathfrak{B}_{r_o}$ the two spacecraft are fully charged and doing their best effort to repel each other. This can be achieved by setting the controller's coefficients k_1 and

k_2 to be some large numbers. Here we set $k_1 = 0.1\text{kgm}^4\text{s/C}^2$, $k_2 = 0.1\text{s/C}$. It can be seen that the larger $q_{\max}$ results in more aggressive repulsion with a larger periapses radius. When $q_{\max} = q_c$, the closest distance is slightly smaller than r_s. Spacecraft 2 penetrates about 0.25m inside the safe restraint region $\mathfrak{B}_{r_s}$ with $r_s = 3$m. This happens because the Debye length effect partially shields the electrostatic force between the spacecraft. But note that 0.25m's penetration is very small compared with r_s, the estimation of the minimum limit charge in Eq. (42) is sufficiently good to provide a very practical maximum required charge computation.

CONCLUSION

This paper discusses a collision avoidance control problem of two spacecraft using Coulomb forces. After formulating the equation of motion of the separation distance, a collision avoidance charge control law with the feedback of the separation distance and the distance rate is developed based on Lyapunov method. The control law is intended to keep the separation distance always greater than a restraint safe radius and also limit changes to the relative kinetic energy. Without charge saturation and truncation, this control works well in fulfilling these two purposes. The control truncations as the craft depart do not influence the accomplishment of a successful collision avoidance, but result in an uncertainty in maintaining the relative kinetic energy. Even though the magnitude of the departure distance rate won't converge asymptotically to the magnitude of the approach rate, the error between these two values is still bounded. The charge saturations may lead to a failure of the collision avoidance control. By ignoring the Debye length effect, analytical conditions under which a potential collision can be prevented are formulated using the gravitational 2-body problem method. Simulation results illustrate the performance of the controller, and show that the controller is robust in preventing collision with control truncation when the spacecraft are flying in GEO. Though the charge limit criteria is not accurate when the Debye length effect is taken into account, the error in predicted minimum separation distance is small.

ACKNOWLEDGMENT

This research is supported by the Virginia Tech ASPIRE program. We also thank Arun Natarajan for assisting with the GEO-based simulation of the charged spacecraft orbits.

REFERENCES

[1] G. L. Slater, S. M. Byram, and T. W. Williams, "Collision Avoidance for Satellites in Formation Flight," *Journal of Guidance, Control, and Dyanmics*, Vol. 29, Sept.-Oct. 2006, pp. 1140–1146.

[2] G. Singh and F. Y. Hadaegh, "Collision Avoidance Guidance for Formation-Flying Applications," *AIAA Guidance, Navigation, and Control Conference and Exhibit*, Aug. 2001.

[3] L. B. King, G. G. Parker, S. Deshmukh, and J.-H. Chong, "Spacecraft Formation-Flying using Inter-Vehicle Coulomb Forces," tech. rep., NASA/NIAC, January 2002. `http://www.niac.usra.edu`.

[4] D. R. Nicholson, *Introduction to Plasma Theory*. Krieger, 1992.

[5] T. I. Gombosi, *Physics of the Space Environment*. Cambridge University Press, 1998.

[6] C. C. Romanelli, A. Natarajan, H. Schaub, G. G. Parker, and L. B. King, "Coulomb Spacecraft Voltage Study Due to Differential Orbital Perturbations," *AAS Space Flight Mechanics Meeting*, Tampa, FL, Jan. 22–26 2006. Paper No. AAS-06-123.

[7] G. G. Parker, C. E. Passerello, and H. Schaub., "Static Formation Control Using Interspacecraft Coulomb Forces.," *2nd International Symposium on Formation Flying Missions and Technologies*, Sept. 14-16 2004.

[8] I. I. Hussein and H. Schaub, "Invariant Shape Solutions of the Spinning Three Craft Coulomb Tether Problem," *AAS Space Flight Mechanics Meeting*, Tampa, Florida, January 22–26 2006. Paper No. AAS 06-228.

[9] G. Parker, L. King, and H. Schaub, "Steered Spacecraft Deployment Using Interspacecraft Coulomb Forces," *American Control Conference*, June 14-16 2006.

[10] A. Natarajan, H. Schaub, and G. G. Parker, "Reconfiguration of a 2-Craft Coulomb Tether," *AAS Space Flight Mechanics Meeting*, Tampa, FL, Jan. 22–26 2006. Paper No. AAS-06-229.

[11] A. Natarajan and H. Schaub, "Linear Dynamics and Stability Analysis of a Coulomb Tether Formation," *AIAA Journal of Guidance, Control, and Dynamics*, Vol. 29, July–Aug. 2006, pp. 831–839.
[12] H. Schaub, G. G. Parker, and L. B. King, "Challenges and Prospect of Coulomb Formations," *Journal of the Astronautical Sciences*, Vol. 52, Jan.–June 2004, pp. 169–193.